Received: 19 November 2018 | Revised: 11 January 2019 | Accepted: 11 January 2019

DOI: 10.1002/er.4404

RESEARCH ARTICLE

WILEY INTERNATIONAL JOURNAL OF ENERGY RESEARCH

Experimental and numerical investigation of heat transfer in Li-ion battery pack of a hoverboard

Abhinav Prasad | Mohammad Parhizi | Ankur Jain

Mechanical and Aerospace Engineering Department, University of Texas at Arlington, Arlington, Texas

Correspondence
Ankur Jain, Mechanical and Aerospace Engineering Department, University of Texas at Arlington, 500 W First St, Rm 211, Arlington, TX, USA 76019 TX.
Email: jaina@uta.edu

Funding information
National Science Foundation, Grant/Award Number: 1554183

Summary

Li-ion cells are used for energy storage and conversion in electric vehicles and a variety of consumer devices such as hoverboards. Performance and safety of such devices are severely affected by overheating of Li-ion cells in aggressive operating conditions. Multiple recent fires and accidents in hoverboards are known to have originated in the battery pack of the hoverboard. While thermal analysis and measurements have been carried out extensively on large battery packs for electric vehicles, there is relatively lesser research on smaller devices such as hoverboards, where the extremely limited thermal management design space and the critical importance of user safety result in severe thermal management challenges. This paper presents experimental measurements and numerical analysis of a novel approach for thermal management of the battery pack of a hoverboard. Measurements indicate that temperature rise in cells in the pack can be as large as 30°C at 4C discharge rate, which, although unlikely to be a standard discharge rate, may result from a malfunction or accident. A novel thermal management approach is investigated, wherein careful utilization of air flow generated by hoverboard motion is shown to result in significant temperature reduction. Measurements also indicate the key role of the metal housing around the battery pack in thermal management. Measurements are found to be in good agreement with finite element simulations, which indicate that the battery pack can be cooled as effectively in presence of a perforated metal casing as without the casing at all. Experimental data and simulation model presented here offer critical insights into the design of hoverboard thermal management and may result in safer, high performance hoverboard battery packs.

KEYWORDS

battery safety, energy storage, hoverboard, lithium ion battery pack, thermal management

1 | INTRODUCTION

Li-ion cells are used for energy storage and conversion in a wide variety of engineering applications such as electric vehicles, grid energy storage, consumer devices, etc.[1-3] Li-ion cells offer greater energy and power density compared with competing technologies,[4] which is particularly important in the case of consumer devices such as cellphones, computing devices, hoverboards, etc in order to maximize battery life while minimizing weight and volume. However, Li-ion cells are also well-known to be very temperature sensitive,[5,6] with a severe reduction

in performance at high temperatures. In addition, overheating of Li-ion cells also presents significant reliability and safety challenges, due to the risk of thermal runaway.[7,8]

A hoverboard is a commonly used, low speed mobility device for individual users. A hoverboard utilizes a battery pack comprising multiple tightly packed Li-ion cells for energy storage. Multiple incidents of fire and explosion in hoverboards have been reported in the recent past, most of which are known to have originated in the battery pack. A systematic investigation of heat transfer in a hoverboard is needed to fully understand and optimize thermal performance and safety of the battery pack. Thermal management of the battery pack of a hoverboard presents challenges because of physical proximity of cells resulting from tight packing, which can cause rapid propagation of thermal runaway due to failure of even a single cell. Further, because of the compact design of the hoverboard and limited power availability, the number of feasible approaches for thermal management is extremely limited.

A significant amount of research has been carried out in order to understand the fundamental heat transfer characteristics of a single Li-ion cell,[7,9-11] as well as battery packs consisting of multiple Li-ion cells.[12-15] At the scale of a single cell, direction-dependent thermal conductivity has been measured.[9,11] Heat generation because of electrochemical reactions inside the cell has been characterized.[16,17] Overall rate of heat generation in the cell has been determined through electrochemical[18] as well as calorimetric[10] measurements. Thermal runaway in a single Li-ion cell has been studied extensively in a variety of abuse conditions,[17,18] through both experiments and theoretical analysis.[7,19]

Much work has also been carried out on thermal measurements and theoretical modeling of battery packs, although most work has been limited to large battery packs of relevance to electric vehicles.[13-15] Active and passive cooling has been investigated through experiments and numerical analysis.[20] Air and liquid-based cooling technique have been studied both experimentally and numerically.[21,22] A water-based hydrogel thermal management approach has been studied to handle the heat surge during the operation of a Li-ion battery pack.[22] The use of liquid cooling plates has also been investigated for battery packs.[23] Phase change material has been used to improve the thermal performance of battery pack in electric scooters.[13,24,25] A combination of aluminum foam and phase change material has been studied for improved heat transfer. A novel hybrid thermal management technique that combines phase change material and forced cooling has been demonstrated for electric vehicle battery pack.[26] Experimental investigation of thermal management of an electric vehicle using heat pipe has been carried out.[27,28] A few research papers have utilized finite element simulations to investigate the thermal performance of a battery pack.[29-31] Numerical modeling of battery pack of laptops by using phase change material has been carried out, and expanded graphite has been impregnated in the phase change material to improve thermal conductivity.[29]

Highlights

- Investigates temperature rise in Li-ion battery pack of a hoverboard through experiments and simulations.
- Shows significant temperature rise and thermal nonuniformity in adverse operating conditions.
- Demonstrates a passive and effective thermal management mechanism by utilizing the flow of air relative to the moving hoverboard.

In contrast to the sizable research on thermal phenomena in large battery packs for electric vehicles summarized above, there is relatively lesser past research on thermal design and management of smaller battery packs for devices such as hoverboards. While the power requirement or total energy stored in a small battery pack such as in a hoverboard may not be as large as an electric vehicle, a systematic study of thermal management of these battery packs is clearly necessitated by the large number of hoverboards in use and the critical need to ensure consumer safety. Further, unlike in an electric vehicle, where active cooling may be feasible, the number of thermal management options are severely limited in a hoverboard because of size and cost considerations. These factors make it critical to optimize heat transfer within these tight constraints in order to minimize peak temperature rise and hence the risk of thermal runaway. A combination of experimental measurements and theoretical/numerical modeling is likely to be an effective approach towards this goal.

This paper presents experimental measurements and numerical analysis of thermal management of the Li-ion battery pack of a hoverboard. The key novelty of this work includes experimental data on baseline thermal performance of a hoverboard that has not been presented in the past, as well as the investigation of a novel thermal management approach for cooling of the battery pack of a hoverboard. A hoverboard is disassembled and instrumented to measure Li-ion cell temperatures during aggressive discharge conditions. Measurements indicate significant temperature rise and risk of thermal runaway

in the present, uncooled condition. Cooling of the battery pack with air flowing relative to the moving hoverboard is investigated by providing cutouts in the hoverboard casing to permit air flow into the battery pack. This, along with removal of a metal casing around the pack is shown to result in 33% reduction in cell temperature rise compared with the present case. Experimental data are found to be in good agreement with results from finite element simulations. Experiments and simulations indicate that the metal casing that houses the battery pack plays a key role in determining the effectiveness of thermal management. The provision of perforations on the casing is shown to result in reasonable reduction in temperature rise without having to completely remove the casing. Experimental data presented here demonstrate the thermal benefit of using the relative speed of air around the moving hoverboard as a passive mechanism for cooling for the battery pack. This does not require any fan work since the air flow is generated due to hoverboard motion. Experimental data on this novel thermal management approach, as well as the numerical simulation model are key contributions of this work that may lead to improved performance and thermal safety of hoverboards.

2 | EXPERIMENTS

It is of interest to measure temperature rise in a battery pack during hoverboard operation. The mobile nature of the hoverboard and lack of physical access to the cells in the battery pack pose challenges in such a measurement. Experiments are designed and carried out to address these challenges and to investigate a novel thermal management strategy to reduce temperature rise in the battery pack.

2.1 | Hoverboard disassembly and instrumentation

The hoverboard is carefully disassembled for obtaining physical access to the battery pack. The plastic panel on the right side of the hoverboard is first removed (Figure 1 A), revealing the battery management system and a metal casing that houses the battery pack (Figure 1B). In order to place thermocouples on cells in the battery pack, the metal casing is carefully removed. To facilitate this, multiple wires that connect the battery management system to the motherboard are cut and reconnected using wire connectors after the metal casing is removed. The battery pack

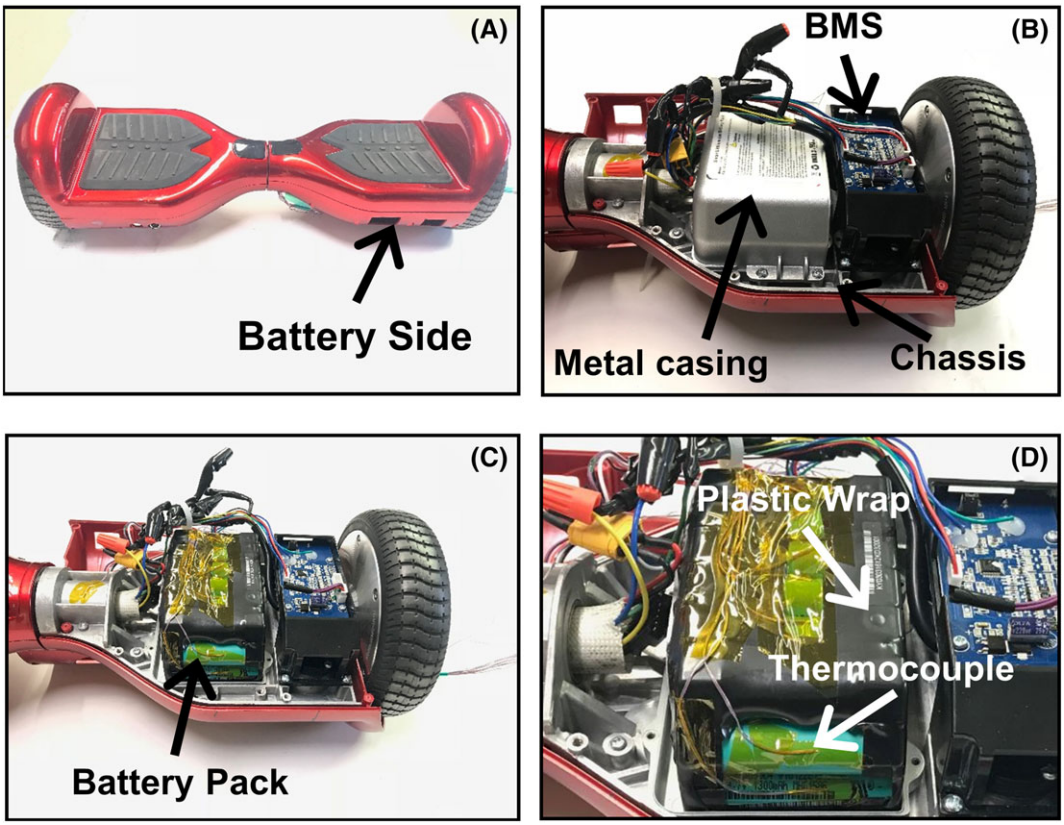

FIGURE 1 A, to C, pictures from disassembly process of the battery pack side of the hoverboard, showing key internal features including metal casing, plastic wrap, and the battery pack. D, Picture showing the instrumentation of cells in the battery pack with thermocouples for temperature measurement during discharge [Colour figure can be viewed at wileyonlinelibrary.com]

inside the casing, shown in Figure 1C, comprises 22 tightly packed 18650 cells that are held together by a thin plastic wrap, also shown in Figure 1C. One face of the cell, insulated by the plastic wrap, touches the metal casing. The assembly of the cells within the battery pack is shown schematically in Figure 2. Note that Figure 2 also schematically shows cutouts for air cooling investigated in experiments and simulations in this work as a means to reduce cell temperature.

There is no active cooling mechanism for the battery pack, which loses heat only through natural convection to the surrounding air and through thermal conduction into the metal casing. The battery pack is not disassembled further since it may not have been possible to assemble it back together. T-type thermocouples of 0.5-mm bead diameter are placed on nine cells that are physically accessible without disassembling the battery pack (Figure 1D). Thermocouple wires are routed out of the metal casing and the outer plastic cover and connected to a National Instruments NI-9213 data acquisition system (DAQ), which is controlled by LabView software running on a 64-bit computer. Temperature data are acquired once every second during the discharge process.

The disassembly and instrumentation of the battery pack with thermocouples reveal key features on the battery side of the hoverboard, such as the metal casing and plastic wrap around the battery pack that play a key role in determining its thermal performance. Information obtained from this process also enables accurate set up of geometrical models for finite element simulations.

2.2 | Hoverboard experimental set up and data acquisition

It is difficult to acquire temperature data from the instrumented thermocouples while the hoverboard is in motion. In order to overcome this challenge and ensure consistent data acquisition in discharge conditions, a roller conveyor set up is designed and fabricated. All measurements are carried out while running the hoverboard on the roller set up. The roller conveyor set up comprises two steel rollers of diameter 35 mm and length 765 mm that are mounted on a rectangular steel frame of dimension 770 mm by 200 mm. The hoverboard is mounted on the rollers during measurements. By rotating the metal rollers, this set up keeps the hoverboard stationary during measurements, which greatly simplifies data acquisition and application of air flow for thermal management. Figure 3A shows a picture of the experimental set up, including the hoverboard mounted on the roller conveyor set up as well as the data acquisition system.

Even though hoverboard motion generates flow of air relative to the hoverboard, this does not directly cool the battery pack, which is difficult for the air flow to access. In order to investigate the potential thermal benefits of the air flow on the battery pack, inlet and outlet grills of dimension 100 mm by 35 mm are cut on the plastic casing of the hoverboard, as shown in Figure 3B. These grills facilitate the flow of air generated due to hoverboard motion into and out of the battery pack. Since the hoverboard in these experiments remains stationary on the roller conveyor set up, this flow of air is mimicked by placing a small fan placed external to the hoverboard. In order to correctly mimic real conditions, air speed from the fan is chosen to match the measured speed of the hoverboard in nominal operating conditions. Air speed is measured directly using a handheld anemometer. The fan is placed about 100 mm from the inlet grill, through which air passes into the inside of the hoverboard. The location of the inlet and outlet grills with respect to the cells in the battery pack is shown schematically in Figure 2. A load of 70 kg is applied on the hoverboard

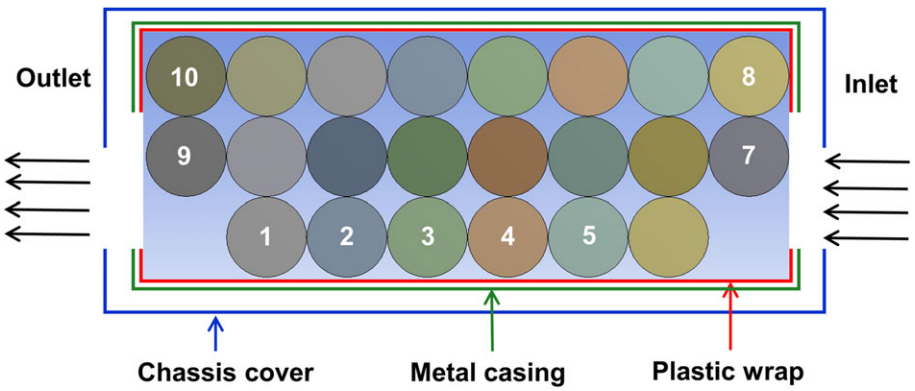

FIGURE 2 Schematic of the assembly of the cells in the battery pack, also showing the plastic wrap and metal casing around the cell assembly, as well as inlet and outlet grills for mimicking the use of air flow generated by hoverboard motion for cooling of the battery pack [Colour figure can be viewed at wileyonlinelibrary.com]

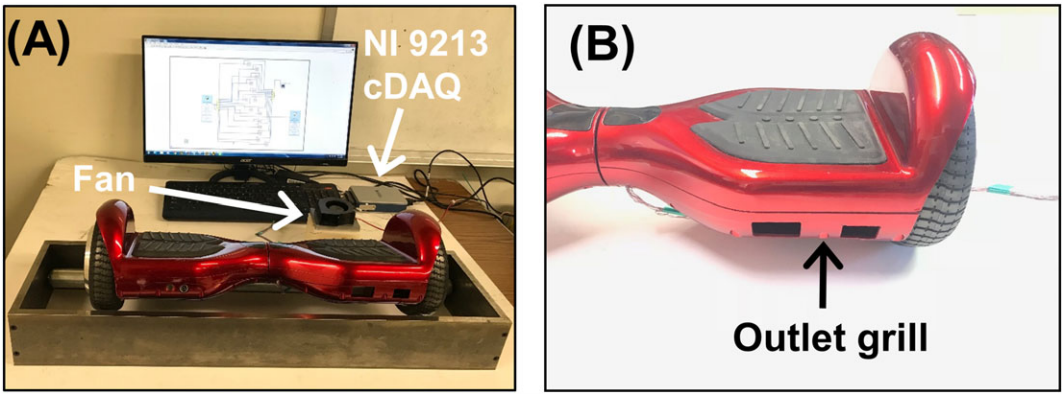

FIGURE 3 A, Picture of the experimental set up showing the hoverboard, cooling fan, and data acquisition set up; B, picture of the outlet grill on the outer plastic body of the hoverboard. The inlet grill, not visible, is on the opposite face [Colour figure can be viewed at wileyonlinelibrary.com]

while it runs at maximum speed on the roller conveyor set up. Operating the hoverboard at the maximum speed may represent the worst-case scenario, with highest heat generation rate that must be dissipated in order to keep the battery pack temperature below thermal runaway threshold. In these experimental conditions, the battery pack is found to discharge completely in 15 minutes, which corresponds to a 4C discharge rate. Experiments are first carried out in baseline conditions without any cooling, which represents the present state-of-the-art. Experiments are also carried out in the presence of cooling air from the external fan that mimics the use of air flow that would be generated by the moving hoverboard in actual conditions.

In summary, this section describes the experimental set up for measurement of temperature rise in the cells of the battery pack of a hoverboard under different operating conditions. These measurements are compared with numerical simulation results, which are discussed in the next section.

3 | NUMERICAL THERMAL MODELING

The transient temperature field in the battery pack of the hoverboard is governed by the following energy conservation equation:

$$\nabla(k\nabla \mathrm{T}) + \dot{Q}''' = \rho C_p \frac{\partial T}{\partial t}, \tag{1}$$

where k is the thermal conductivity, which can in general be anisotropic,[9] ρ and C_p are density and heat capacity respectively and $\dot{Q}'''$ is the internal heat generation rate. Temperature and heat flux continuity are applicable at interfaces between different materials. Finally, a convective heat transfer boundary condition is applicable on the outer surfaces of the geometry

$$k\nabla \mathrm{T} = h(T - T_\infty), \tag{2}$$

where h is the convective heat transfer coefficient and T_∞ is the ambient temperature.

Because of the complex geometry of the battery pack, a closed form, analytical solution of the temperature field is not possible. Instead, the transient temperature field in the battery pack and hoverboard during operation is computed by numerically solving for the temperature field using the finite element method in a commercial software tool. The key heat transfer phenomena modeled here include volumetric heat generation in each Li-ion cell during discharge, anisotropic thermal conduction within the cells, thermal conduction through the various components of the battery pack and hoverboard, and finally, convective heat transfer to surrounding air. Simulations did not compute the electrochemistry within the cell since the discharge rate, and therefore, heat generation rate is taken to be constant through the discharge period.[10]

Key thermal parameters that influence the temperature field in the hoverboard include heat generation rate and thermal properties of the cells. A 4C discharge rate is used, which matches the experiments described in the previous section. Heat generation rate corresponding to this discharge rate is determined based on past measurements on the same type of cell.[10] Heat generation rate is assumed to be constant throughout the discharge process. The value of volumetric heat generation rate is obtained from past measurements,[10] in which the heat generation rate was determined at multiple discharge rates for a similar cylindrical cell of the same electrochemistry as the present cell. In this paper, the heat generation rate was measured by adding up the total heat lost from the cell surface and energy stored within the cell.[10] These were, in turn, measured using a heat flux sensor attached on the cell surface and thermocouples to measure temperature rise in the cell.[10] It is assumed that at the

same discharge rate, the volumetric heat generation rate is the same between the cell types in the cited work and the present work. This is a reasonable assumption since both cells employ the same electrochemistry for energy storage and conversion. Thermal conductivity of the Li-ion cells is taken to be 0.20 and 30.4 W/mK in the radial and axial directions respectively, based on past measurements on 18650 Li-ion cells,[9] which is the same cell type as used in the hoverboard.

The geometry of the hoverboard is obtained from measurements on the disassembled hoverboard. Natural convection cooling with a convective heat transfer coefficient of 10 W/m^2K is assumed for boundary conditions on the outer surfaces for simulations of cases with no forced air. For forced air cooling, fluid flow is modeled with a velocity boundary condition at the inlet. The inlet air speed is obtained from direct measurements from an anemometer. A mesh of 857307 nodes is utilized for finite element computations. As shown in Figure 4, further mesh refinement is found to produce negligible change in the computed temperature field, thereby establishing mesh independence.

In summary, this section discusses the details of the finite element simulations carried out for understanding heat transfer in the Li-ion battery pack of the hoverboard. Comparison with experimental measurements is discussed in the next section.

4 | RESULTS AND DISCUSSION

4.1 | Temperature measurements

Figure 5 presents measured temperature rise at the surface of four cells in the battery pack during an aggressive hoverboard operation at 4C discharge rate. Positions of

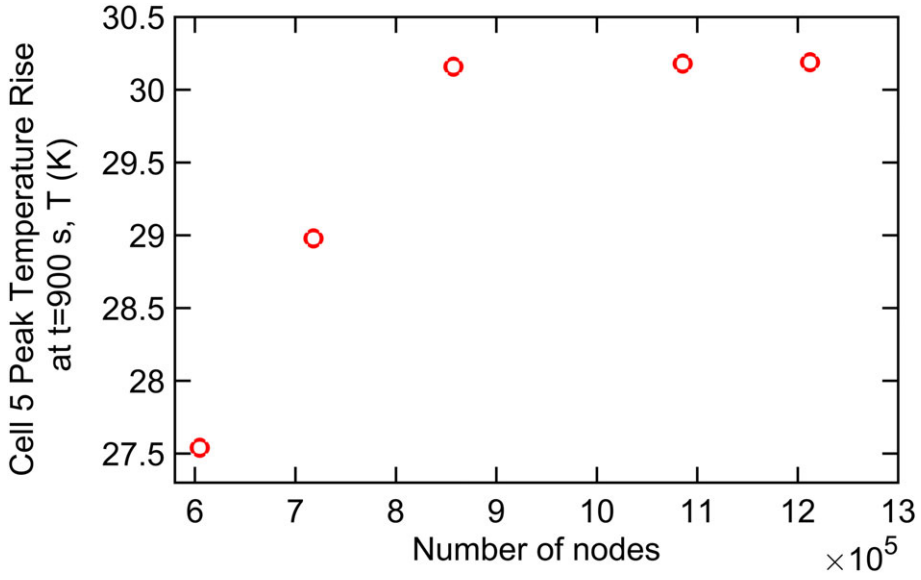

FIGURE 4 Plot of peak temperature in cell 5 at the end of discharge period predicted by finite element simulations as a function of number of nodes in the simulation [Colour figure can be viewed at wileyonlinelibrary.com]

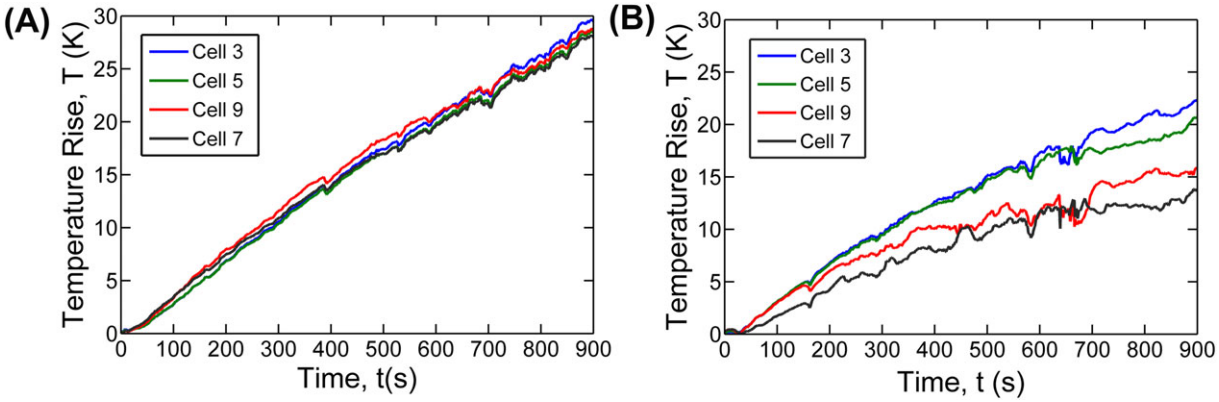

FIGURE 5 Experimental measurement of temperature rise as a function of time in four cells of the battery pack during discharge at 4C rate. Measurements are shown in A, free convection and B, air cooled conditions [Colour figure can be viewed at wileyonlinelibrary.com]

the cells within the battery pack are shown in Figure 2. Measurements are presented in two distinct cases. Figure 5A plots temperature for free convection conditions, wherein there is no forced air cooling, and the cells are cooled only by free convection to the air around the battery pack. Figure 5B plots temperature in a similar discharge process when the pack is cooled by relative air flow, mimicked by an external fan, as shown in Figure 3A. Figure 5A shows, as expected, increasing temperature with time while the discharge process proceeds to completion. There is nearly uniform temperature rise among all four measured cells. The cell surface temperature increases by about 30°C, which is a significant temperature rise. Such a large temperature rise is likely to cause performance and safety problems, particularly in a hot climate since the manufacturer-specified safe temperature threshold for Li-ion cells is often only around 60°C to 70°C. Even though a well-designed battery management system is expected to limit the discharge rate in order to limit temperature rise, malfunction, poor design, or operation in a challenging ambient may lead to the temperature rise measured here.

In contrast with Figure 5A, experiments that mimic the cooling of the battery pack with air flow generated by hoverboard motion show substantial temperature reduction, as plotted in Figure 5B. The benefit is particularly significant for cells 7 and 9, which are located in the leading edge and trailing edge regions, respectively. Peak temperature rises during forced convection reduces by half for cells 7 and 9 compared with the baseline case, which is a very significant reduction. While cell 7 benefits from direct impingement of the cooling air, the significant temperature reduction in cell 9 likely occurs due to air recirculation in the back of the battery pack. Cells 3 and 5, which are located on the side of the battery pack also benefit from cooling, although the benefit is lesser than cells 7 and 9.

Note that the four cells for which data are reported in Figure 5 represent different locations in the battery pack with respect to the cooling air flow. Temperature measurement for other cells, particularly those located in the inner region of the pack is not possible due to lack of accessibility. Temperature for such cells may be obtained from experimentally validated finite element simulations as discussed in section 4.2. Further, data reported here are all surface temperatures, whereas the core temperature may be much greater.[19] Section 4.4 later estimates the core temperature based on these measurements using a recently developed analytical model.[19,32]

These experimental data establish the fundamental thermal benefit of using the air flow generated by hoverboard motion for cooling the battery pack. In harsh conditions, such as aggressive hoverboard operation in a high temperature ambient, the thermal benefit shown in Figure 5B may be sufficient enough to prevent thermal runaway or at least improve device reliability significantly. Note that the convective cooling benefits shown here has not been optimized much in this study. Even greater temperature reduction than reported here may be possible, for example, by making the cell arrangement within the battery pack more aerodynamic. This is difficult to investigate in this work due to the lack of flexibility in making such changes in a commercial hoverboard.

4.2 | Simulation results and comparison with experimental data

It is clearly desirable to develop a finite element simulation model for the temperature distribution in the hoverboard. This becomes particularly important because several cells in the battery pack are difficult to access for direct temperature measurement and, also because the internal temperature of a cell is not possible to measure because of its hermetically sealed nature. In such a case, a model that predicts temperature inside the pack by accounting for the geometry of the battery pack and cooling conditions may be a valuable design tool. Validation of such a model against experimental data is critical as it increases confidence in model predictions.

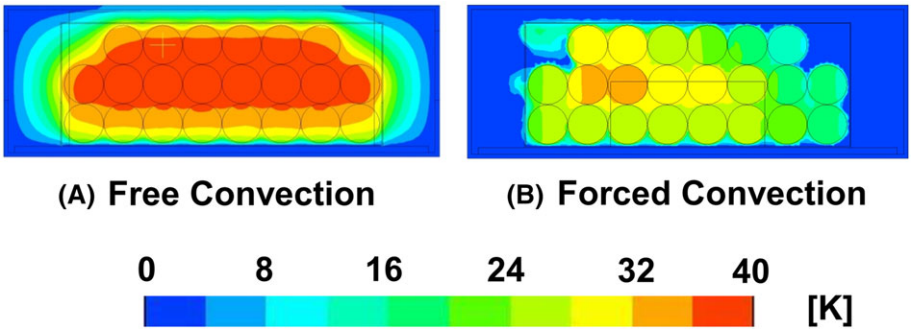

FIGURE 6 Colormap of temperature rise in the battery pack during discharge at 4C rate based on finite element simulations for A, free convection and B, air cooled conditions [Colour figure can be viewed at wileyonlinelibrary.com]

Figure 6 presents a colormap of temperature distribution in the battery pack at the end of a 4C discharge rate in two different cooling conditions based on finite element simulations described in section 3. When the hoverboard operates in free convection conditions, significant temperature rise occurs in each cell of the battery pack, as shown in Figure 6A. Temperature field is quite uniform among all cells, which is consistent with experimental data shown in Figure 5A. The use of air flow generated by hoverboard motion results in substantial temperature reduction, as shown in Figure 6B. There is some nonuniformity in the temperature map in this case, depending on cell location within the battery pack with respect to air flow. The improved temperature field in the battery pack may contribute towards reduced risk of thermal runaway, as well as improved performance since the reduced pack temperature can be leveraged to increase the discharge rate of the pack. However, the intercell nonuniformity induced because of convective cooling must also be accounted for by the battery management system.

Figure 7 presents comparison of experimentally measured temperature rise as a function of time with finite element simulation results for four cells in the battery pack. Comparison is presented for both free convection conditions as well as forced convective cooling through a small fan. Both experimental measurement and simulation results follow similar trends for each cell, and in each case, good agreement between the two is observed. The RMS error between the two over the entire discharge period is found to be 13.7%, 13.8%, 12.2%, and 12.5% for cells 3, 5, 7, and 9 respectively for the case without fan. In the presence of the fan, these errors are 14.4%, 10.9%, 27.0%, and 13.7%. The large RMS error in the case of cell 7 with fan is likely because, as shown in Figure 2, this cell directly faces the impinging flow, which might lead to larger fluctuations in temperature. Temperature rise is lower for forced convection cooling compared with free convection for each cell, as expected. Note that the four cells for which results are presented in Figure 7 are ones that were easily accessible during experiments for mounting thermocouples. These cells represent distinct flow regions with respect to the inlet coolant air flow. While coolant air impinges directly on cell 7, cell 9 is located closer to the outlet grill, and cells 3 and 5 are located on the side. The good agreement between simulation results and experimental data in different conditions for different cells validates the simulation model as a useful thermal design tool for understanding and optimizing the thermal characteristics of a hoverboard battery pack. For example, once validated, the model is capable of accurately predicting temperature for cells that are difficult to measure directly, such as cells in the interior of the battery pack.

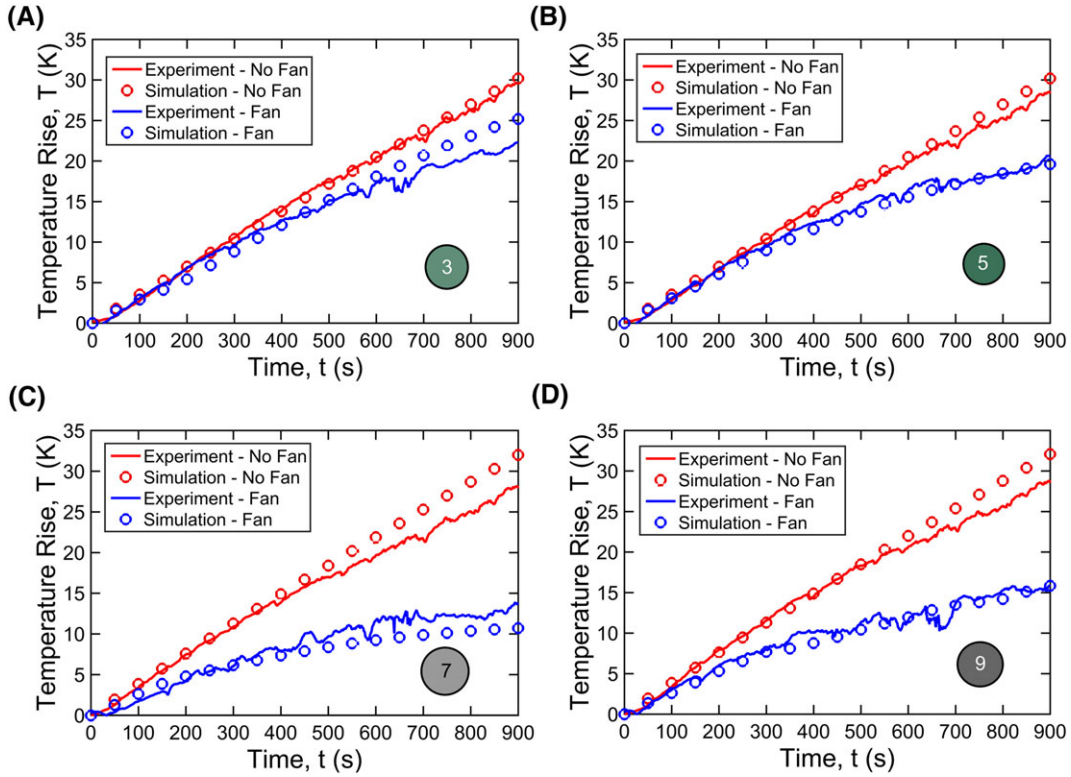

FIGURE 7 Comparison of experimentally measured temperature rise as a function of time with finite element simulation predictions for discharge at 4C rate. Comparison is shown for four different cells in the battery pack and for two different cooling conditions [Colour figure can be viewed at wileyonlinelibrary.com]

The experimentally validated simulation model is capable of predicting thermal performance of the hoverboard battery pack in a variety of operating conditions. Figure 8 plots temperature rise in cell 5 as a function of time for multiple discharge rates in two different cooling conditions. These plots show that the cell temperature increases rapidly with increasing C-rate. In general, the greater the C-rate, the higher is the performance of the hoverboard. Plots such as Figure 8 help develop a trade-off between performance and thermal safety of the hoverboard battery pack.

4.3 | Effect of metal casing on thermal management

The battery pack in the hoverboard is protected from external impact and abuse by a metal casing, as shown in Figure 1B. However, it is likely to adversely impact forced convection cooling of cells in the battery pack by physically isolating the cells from the air flow. A set of experiments is carried out to examine this challenge in detail and propose a possible solution.

Figure 9 plots temperature of cell 5 measured as a function of time during 4C discharge for three different conditions related to the metal casing. As a baseline, temperature in presence of the metal casing and with no air flow is plotted. This represents the present state-of-the-art in a hoverboard battery pack, wherein the cells in the pack cool down only through natural convection. Temperature is also plotted for the case of air flow with the metal casing present. A comparison of these two plots shows that while air flow from the fan reduces temperature rise, the effect is not significant, primarily because the presence of the metal casing prevents direct impingement of air flow on the cells and therefore severely limits the benefit of convective cooling. Experimental data are also plotted in Figure 9

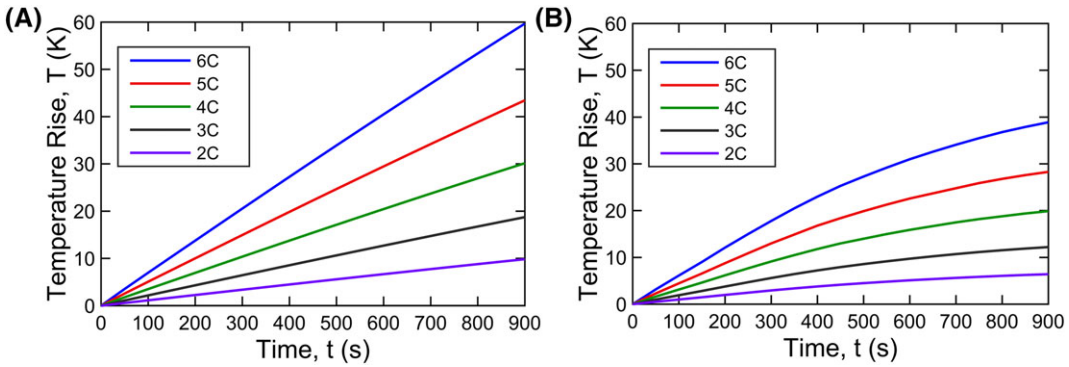

FIGURE 8 Plots of temperature rise of cell 5 as a function of time for multiple discharge rates in A, free convection conditions and B, air cooled conditions [Colour figure can be viewed at wileyonlinelibrary.com]

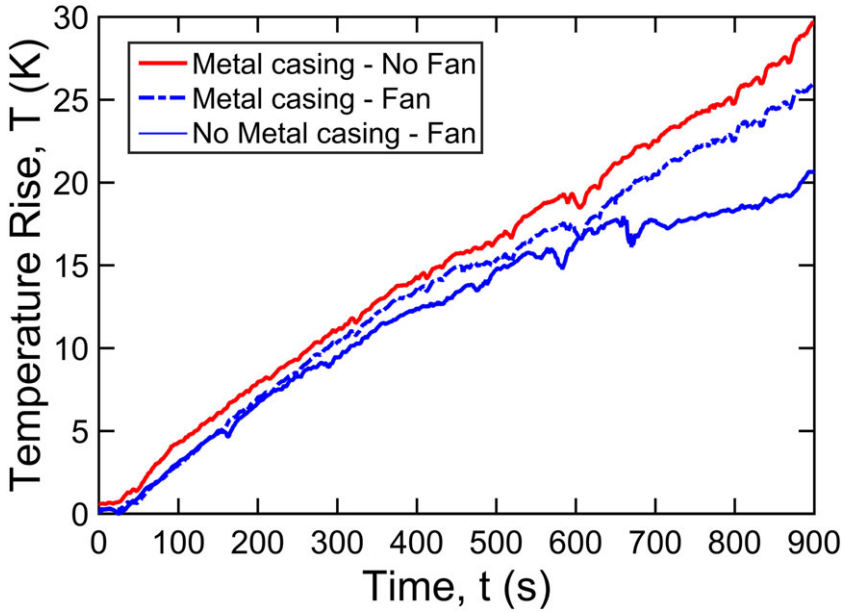

FIGURE 9 Experimentally measured temperature rise in cell 5 as a function of time for the baseline case and for air cooling without and with the metal casing, showing that the effect of cooling is more pronounced in the absence of the metal casing, which facilitates direct air impingement on the battery pack [Colour figure can be viewed at wileyonlinelibrary.com]

for the case where the metal casing is removed completely in addition to providing air flow. A significantly greater thermal benefit is obtained in this case, with a nearly 33% reduction in measured temperature at the end of the discharge process compared with the baseline case. Finite element simulations of these cases confirm, as expected, that the removal of the metal casing facilitates direct impingement of coolant flow on the cells in the battery pack and therefore, more effective cooling.

Despite the significant thermal benefit of removing the metal casing completely, it may not always be possible to do so because the casing protects the battery pack from external impacts and possibly also serves a structural function. As an alternative to completely removing the metal casing, the possibility of providing greater air flow into the battery pack through perforations in the metal casing is investigated through simulations. Figure 10 plots temperature rise in cell 5 during 4C discharge for the baseline case of no fan based on finite element simulations. In addition, simulation results for the thermally beneficial but perhaps impractical case of removing the metal casing completely while providing air flow is also plotted. For comparison, finite element simulations are carried out for the case where two perforations of dimension 55 mm by 35 mm are provided on the front and back surfaces of the metal casing. Temperature distribution for this case, also plotted in Figure 10 clearly shows that the thermal benefit in this case is nearly as much as the case where the metal casing is removed completely. This may present a reasonable compromise in designing thermal management of the battery pack while keeping the metal casing in place. Perforations in the metal casing permit significant air flow to the battery pack without adversely impacting the structural function of the casing.

Table 1 summarizes key results presented in Figures 9 and 10. Temperature rise for four cells in the battery pack at the end of a 4C discharge process is reported for three cases—the present state-of-the-art, baseline case with no air cooling, air cooling with no metal casing around the battery pack, and air cooling with a perforated metal casing. Table 1 shows significant reduction in temperature rise as a result of air cooling. Further, Table 1 also shows a nearly similar thermal benefit of having a perforated metal casing compared with no metal casing at all. As

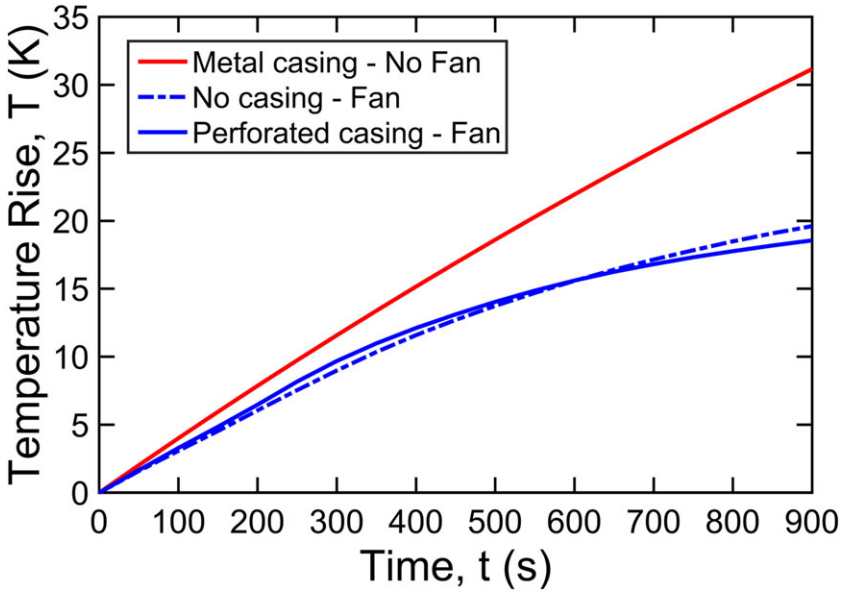

FIGURE 10 Temperature rise as a function of time in cell 5 during discharge at 4C discharge rate based on finite element simulations. Comparison is shown between the baseline case, air cooling without the metal casing at all, and air cooling with a perforated metal casing [Colour figure can be viewed at wileyonlinelibrary.com]

TABLE 1 Peak temperature rise at the end of 4C discharge in four cells in the battery pack for the baseline case, air cooling case with no metal casing, and air cooling case with a perforated metal casing

Cell	Baseline Case—No Cooling (Experiment)	Air Cooling with no Metal Casing (Experiment)	Air Cooling with Perforated Metal Casing (Simulation)
Cell 3	29.9	22.1	25.1
Cell 5	29.5	20.5	18.3
Cell 7	28.7	13.4	11.5
Cell 9	28.7	15.6	15.5

discussed earlier, these thermal benefits are obtained without the need for any pumping power since the air flow is generated simply by the relative motion of hoverboard through the air.

4.4 | Core temperature computation and temperature nonuniformity in battery pack

Because of the hermetically sealed nature of a Li-ion cell, most experiments, including those described in section 4.1, are able to report only the surface temperature measured by a thermocouple attached on the outer surface of the cell. Because of the low radial thermal conductivity of the cell,[9] however, it is likely that the core temperature may be much greater and therefore may play a more significant role than the surface temperature in determining the safety of the cell.[19,32] For example, when a surface temperature measurement indicates somewhat elevated temperature, the core temperature may in fact be much greater because of internal heat generation and large thermal conduction resistance within the cell. Therefore, thermal management decisions based on the surface temperature may not fully recognize the possibility of thermal runaway. In order to investigate this for the specific case of the hoverboard in this work, the core temperature of cell 5 is determined based on surface temperature measurements without and with cooling fan. A recently reported model[19,32] solves the underlying energy conservation equations to determine the core temperature as a function of time using the surface temperature measurements as an input. Internal heat generation rate and radial thermal conductivity of the cell are also utilized as inputs into the model. Results presented in Figure 11 indicate that the core temperature is significantly elevated compared with the surface temperature in both cases. The mismatch between surface and core temperature is found to be greater when a fan is provided. This happens because of reduced convective thermal resistance external to the cell in the presence of air flow, which makes the conduction resistance relatively more significant and thereby increases the difference between core and surface temperatures. Results presented in Figure 11 indicate that it is important to recognize the elevated core temperature with respect to surface temperature, particularly when the battery pack of the hoverboard is being actively cooled.

Spatial nonuniformity of temperature is also important to recognize at the pack level. As shown in Figure 6, forced air cooling reduces peak temperatures in the battery pack but also increases temperature nonuniformity between various cells in the pack. Cells closer to air flow are clearly cooler than those located in the inner regions of the pack where there is no direct air flow.

A key trade-off to be considered in the cooling of the battery pack is the balance between peak temperature rise and spatial thermal uniformity. An effective external cooling mechanism, such as the one discussed here, may reduce the external cell temperature but not necessarily cool the core of the cell, thereby resulting in a thermal imbalance within the cell. A combination of internal and external cooling may be needed for effective cooling that reduces both temperature rise and temperature gradient within the cell.

In summary, this section shows good agreement between experimental measurements and finite element simulations. Interesting predictions for thermal management of the battery pack based on simulations, as well

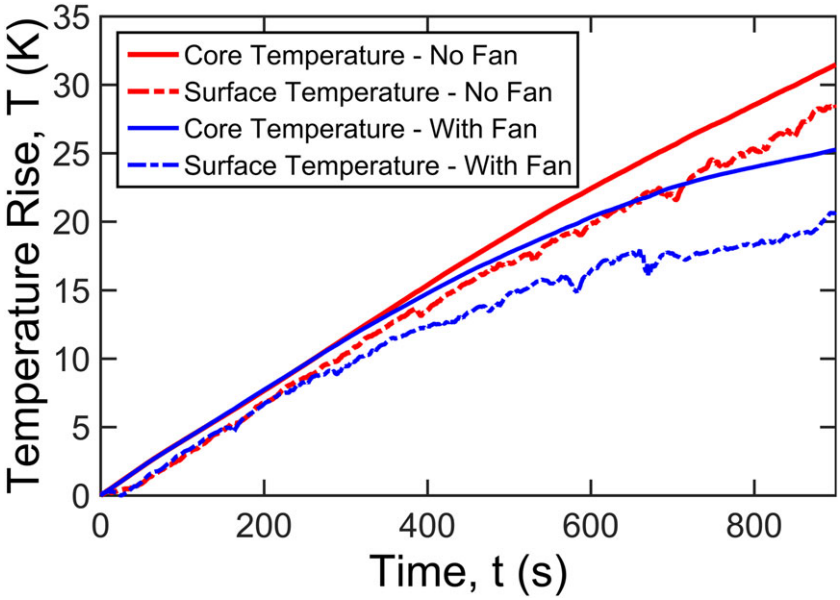

FIGURE 11 Comparison of measured surface temperature and predicted core temperature in cell 5 as functions of time during discharge at 4C rate for two different cooling conditions. Results indicate significant temperature gradient within the cell, particularly during air cooling [Colour figure can be viewed at wileyonlinelibrary.com]

as a novel, passive thermal management approach have also been described.

5 | CONCLUSIONS

Results discussed above present critical insights into heat transfer processes in the battery pack of a hoverboard. Multiple recent fires and accidents in hoverboards are known to have originated in the battery pack of the hoverboard. While hoverboards have not received as much research attention as electric vehicles, ensuring the safety of hoverboards is nevertheless very critical because of their widespread use and the limited available thermal management design space. Experimental measurements presented here highlight the importance of active cooling, particularly in aggressive operating conditions. Cooling with the air stream around the hoverboard during motion is mimicked in experiments and is shown to result in significant temperature reduction, with the possibility of even greater benefit through flow and thermal optimization. Even though an external fan is used in this work to mimic this air flow, in real conditions, the flow will be generated by the hoverboard motion without the need of an external fan and associated power input. Experimental data also highlight the important role of the metal casing around the battery pack in thermal management. These results also indicate a trade-off between thermal management and structural function of the metal casing wherein a perforated casing may offer extensive thermal benefit without compromising its structural function. The experimentally validated simulation models discussed in this work offer a useful design tool for battery pack thermal management in a hoverboard. Thermal optimization based on such a tool may lead to safer, higher performance hoverboards.

ACKNOWLEDGEMENT

This material is based upon work supported by CAREER Award No. CBET-1554183 from the National Science Foundation.

ORCID

Ankur Jain https://orcid.org/0000-0001-5573-0674

REFERENCES

1. Shah K, Balsara N, Banerjee S, et al. State of the art and future research needs for multiscale analysis of Li-ion cells. *J Electr Energy Conv Storage*. 2017;14(2):020801. https://doi.org/10.1115/1.4036456
2. Scrosati B, Garche J. Lithium batteries: status, prospects and future. *J Power Sources*. 2010;195(9):2419-2430. https://doi.org/10.1016/j.jpowsour.2009.11.048
3. Etacheri V, Marom R, Elazari R, Salitra G, Aurbach D. Challenges in the development of advanced Li-ion batteries: a review. *Energ Environ Sci*. 2011;4(9):3243. https://doi.org/10.1039/C1EE01598B
4. Linden D, Reddy TB. *Handbook of Batteries*. 3rd ed. New York: McGraw-Hill; 2002.
5. Shah K, Vishwakarma V, Jain A. Measurement of multiscale thermal transport phenomena in Li-ion cells: a review. *J Electr Energy Conv Storage*. 2016;13(3):030801. https://doi.org/10.1115/1.4034413
6. Bandhauer TM, Garimella S, Fuller TF. A critical review of thermal issues in Lithium-ion batteries. *J Electrochem Soc*. 2011;158. https://doi.org/10.1149/1.3515880
7. Shah K, Chalise D, Jain A. Experimental and theoretical analysis of a method to predict thermal runaway in Li-ion cells. *J Power Sources*. 2016;330:167-174. https://doi.org/10.1016/j.jpowsour.2016.08.133
8. Lopez CF, Jeevarajan JA, Mukherjee PP. Characterization of Lithium-ion battery thermal abuse behavior using experimental and computational analysis. *J Electrochem Soc*. 2015;162. https://doi.org/10.1149/2.0751510jes
9. Drake S, Wetz D, Ostanek J, Miller S, Heinzel J, Jain A. Measurement of anisotropic thermophysical properties of cylindrical Li-ion cells. *J Power Sources*. 2014;252:298-304. https://doi.org/10.1016/j.jpowsour.2013.11.107
10. Drake S, Martin M, Wetz D, et al. Heat generation rate measurement in a Li-ion cell at large C-rates through temperature and heat flux measurements. *J Power Sources*. 2015;285:266-273. https://doi.org/10.1016/j.jpowsour.2015.03.008
11. Zhang J, Wu B, Li Z, Huang J. Simultaneous estimation of thermal parameters of large- format laminated Lithium-ion batteries. *J Power Sources*. 2014;259:106-116. http://doi.org/10.1016/j.jpowersour.2014.02.079
12. Lopez CF, Jeevarajan JA, Mukherjee PP. Evaluation of combined active and passive thermal management strategies for Lithium-ion batteries. *J Electr Energy Conver Storage*. 2016;13(3):031007. http://doi.org/10.1115/1.4035245
13. Khateeb SA, Amiruddin S, Farid M, Selman JR, Hallaj SA. Thermal management of Li-ion battery with phase change material for electric scooters: experimental validation. *J Power Sources*. 2005;142(1-2):345-353. https://doi.org/10.1016/j.jpowsour.2004.09.033
14. Zolot M.D., Kelly K., Keyser M., Mihalic M., Pesaran A, Hieronymus A., "Thermal evaluation of the Honda Insight battery pack", In: 36th ASME Intersoc. Energy Conv. Eng. Conf., 2001, pp. 923.
15. Zolot M, Pesaran A, Mihalic M. *Thermal Evaluation of Toyota Prius Battery Pack*. Virginia, USA: Proc. Future Car Congress; 2002.
16. Macneil D, Lu Z, Chen Z, Dahn J. A comparison of the electrode/electrolyte reaction at elevated temperatures for various Li-ion battery cathodes. *J Power Sources*. 2002;108(1-2):8-14. https://doi.org/10.1016/S0378-7753(01)01013-8

17. Spotnitz R, Franklin J. Abuse behavior of high-power, lithium-ion cells. *J Power Sources*. 2003;113(1):81-100. https://doi.org/10.1016/S0378-7753(02)00488-3

18. Golubkov AW, Fuchs D, Wagner J, et al. Thermal-runaway experiments on consumer Li-ion batteries with metal-oxide and olivin-type cathodes. *RSC Adv*. 2014;4(7):3633-3642. https://doi.org/10.1039/C3RA45748F

19. Parhizi M, Ahmed M, Jain A. Determination of the core temperature of a Li-ion cell during thermal runaway. *J Power Sources*. 2017;370:27-35. https://doi.org/10.1016/j.jpowsour.2017.09.086

20. Karimi G, Li X. Thermal management of lithium-ion batteries for electric vehicles. *Int J Energ Res*. 2012;37:13-24. https://doi.org/10.1002/er.1956

21. Qian Z, Li Y, Rao Z. Thermal performance of lithium-ion battery thermal management system by using mini-channel cooling. *Energ Convers Manag*. 2016;126:622-631. https://doi.org/10.1016/j.enconman.2016.08.063

22. Zhao R, Zhang S, Gu J, Liu J, Carkner S, Lanoue E. An experimental study of lithium ion battery thermal management using flexible hydrogel films. *J Power Sources*. 2014;255:29-36. https://doi.org/10.1016/j.jpowsour.2013.12.138

23. Zhao J, Rao Z, Li Y. Thermal performance of mini-channel liquid cooled cylinder based battery thermal management for cylindrical lithium-ion power battery. *Energ Conver Manage*. 2015;103:157-165.

24. Khateeb SA, Farid MM, Selman J, Al-Hallaj S. Design and simulation of a lithium-ion battery with a phase change material thermal management system for an electric scooter. *J Power Sources*. 2004;128(2):292-307. https://doi.org/10.1016/j.jpowsour.2003.09.070

25. Parhizi M, Jain A. Analytical modelling and optimization of phase change thermal management of Li-ion battery pack. *Appl Therm Eng*. 2019;148:229-237.

26. Ling Z, Wang F, Fang X, Gao X, Zhang Z. A hybrid thermal management system for lithium ion batteries combining phase change materials with forced-air cooling. *Appl Energy*. 2015;148:403-409. https://doi.org/10.1016/j.apenergy.2015.03.080

27. Rao Z, Wang S, Wu M, Lin Z, Li F. Experimental investigation on thermal management of electric vehicle battery with heat pipe. *Energ Conver Manage*. 2013;65:92-97. https://doi.org/10.1016/j.enconman.2012.08.014

28. Ye Y, Shi Y, Saw LH, Tay AA. Performance assessment and optimization of a heat pipe thermal management system for fast charging lithium ion battery packs. *Int J Heat Mass Transfer*. 2016;92:893-903. https://doi.org/10.1016/j.ijheatmasstransfer.2015.09.052

29. Mills A, Hallaj SA. Simulation of passive thermal management system for lithium-ion battery packs. *J Power Sources*. 2005;141(2):307-315. https://doi.org/10.1016/j.jpowsour.2004.09.025

30. Hallaj SA, Maleki H, Hong JS, Selman JR. Thermal modeling and design considerations of lithium-ion batteries. *J Power Sources*. 1999;83:1-8. https://doi.org/10.1016/S0378-7753(99)00178-0

31. Ye Y, Saw LH, Shi Y, Tay AA. Numerical analyses on optimizing a heat pipe thermal management system for lithium-ion batteries during fast charging. *Appl Thermal Eng*. 2015;86:281-291. https://doi.org/10.1016/j.applthermaleng.2015.04.066

32. Anthony D, Wong D, Wetz D, Jain A. Non-invasive measurement of internal temperature of a cylindrical Li-ion cell during high-rate discharge. *Int J Heat Mass Transfer*. 2017;111:223-231. http://doi.org/10.1016/j.ijheatmasstransfer.2017.03.095

How to cite this article: Prasad A, Parhizi M, Jain A. Experimental and numerical investigation of heat transfer in Li-ion battery pack of a hoverboard. *Int J Energy Res*. 2019;43:1802–1814. https://doi.org/10.1002/er.4404